

SIMULATION AND SYMMETRY IN MOLECULAR DIFFUSION AND SPECTROSCOPY

M. W. EVANS

*Center for Theory and Simulation in Science and Engineering,
Cornell University, Ithaca, New York*

CONTENTS

Introduction

- I. The Traditional View
 - A. Einstein's Theory of Translational Brownian Motion
 - B. The Langevin Equation for Translational Brownian Motion
 - C. Contemporary Criticism of the Traditional Approach
 - D. Molecular Translation and Rotation
 - E. Dielectric Relaxation and the Debye Theory of Rotational Diffusion
 - F. Loss of Polarization
 - G. The Concept of Rotational Diffusion
 - H. Rise Transient
 - I. The Fall Transient
 - J. Polarization and Frequency Spectrum
 - K. Dielectric and Far Infrared Spectrum
 - L. The Debye Plateau
 - M. Far Infrared Interferometry
 - N. The Effect of Including the Inertial Term in Eq. (8)
 - O. Rotational Diffusion in a Potential Well: The Itinerant Oscillator
 - P. The Harmonic Approximation
 - Q. The Itinerant Oscillator
 - R. Experiment Testing of the Itinerant Oscillator
 - S. Relationship of the Itinerant Oscillator with the Liouville Equation
 - T. The Grigolini Continued Fraction
 - U. The Statistical Correlation between Rotation and Translation
 - V. The Challenge to Traditional Diffusion Theory
- II. Key Experiments
 - A. Interferometric Spectroscopy of Molecular Liquids

- B. The Basic Principles of Fourier Transform Spectroscopy in the Far Infrared
 - C. The Interferogram
 - D. Key Spectral Data: The Challenge to Diffusion Theory
 - E. Condensation of Gas to Liquid
 - F. The Molecular Liquid at Room Temperature and Pressure
 - G. Molecular Dynamics Simulation
 - H. From Liquid to Glass at Constant Pressure
 - I. The Challenge to Computer Simulation
 - J. Survey of Data for Liquid Dichloromethane
 - K. The Relaxation of Nuclear Magnetic Resonance
 - L. The Challenge to the Theory of NMR Relaxation
 - M. Anisotropy of Diffusion in the Asymmetric Top
 - N. Light Scattering
 - O. Raman Scattering
 - P. The Challenge to the Traditional Approach to Light Scattering
 - Q. Neutron Scattering
 - R. Infrared Absorption
 - S. The Role of Computer Simulation in Data Coordination
 - T. Dielectric Relaxation and Far Infrared Absorption
- III. Computer Simulation
- A. Summary of Numerical Approximations
 - B. Periodic Boundary Conditions
 - C. Numerical Integration of the Equations of Motion
 - D. The Gear Predictor-Corrector
 - E. The Leapfrog Algorithm
 - F. Integration of the Rotational Equations
 - G. Other Molecular Dynamics Simulation Algorithms
 - H. Rahman's Computer Simulation of Liquid Argon
 - I. Some Fundamental Properties of Time Correlation Functions
 - J. The Long Time Tail
 - K. The Interaction between Rotational and Translational Molecular Diffusion
 - L. Simulation of Liquid Dichloromethane
 - M. Comparison of Simulation with Spectral Data
 - N. The Lennard-Jones Atom-Atom Potential for Dichloromethane
 - O. Computer Simulation Methods
 - P. Some Tests for the Liquid State
 - Q. Thermodynamic Properties
 - R. Thermodynamic Results for Dichloromethane
 - S. Dynamical and Spectral Properties
 - T. Microwave and Far Infrared Absorption and Dispersion
 - U. Infrared Absorption
 - V. Relaxation of Nuclear Magnetic Resonance
 - W. Depolarized Rayleigh Scattering
 - X. Incoherent, Inelastic Neutron Scattering
 - Y. Survey of Correlation Times
 - Z. A Survey of Molecular Liquids
- IV. Simulation—New Results
- A. Linear Response Theory and the Fluctuation-Dissipation Theorem

- B. Taylor Expansion of the Smoluchowski Equation
 - C. The Concept of Linear Response
 - D. Rotational Diffusion
 - E. Solution for Arbitrary Field Strength
 - F. Computer Simulation of Rise and Fall Transients in an Arbitrarily Strong External Field—Violation of the Linear Response Theory
 - G. Computer Simulation in an Applied External Field
 - H. Rise Transients
 - I. The Langevin Function
 - J. Time Dependence of the Rise Transient
 - K. The Fall Transient
 - L. Correlation Functions in the Field on Steady State
 - M. The Decoupling Effect
 - N. New Types of Birefringence
 - O. The Kerr Effect
 - P. The Cotton-Mouton Effect
 - Q. Birefringence Induced with Electromagnetic and Neutron Radiation
 - R. Flow-Induced Birefringence
 - S. Birefringence Effects Discovered by Computer Simulation
 - T. Electric-Field-Induced Translational Anisotropy
 - U. Birefringence Induced by a Circularly Polarized Laser
 - V. Computer Simulation of Birefringence due to Circular Flow
 - W. Field Equations for Circular Flow
 - X. Anisotropy in Linear Diffusion Produced by a Circularly Polarized Laser
 - Y. Electric or Circularly Polarized Laser Field Applied to a Dilute Gas
 - Z. Correlation between Rotation and Translation Induced by Electric Fields
 - AA. Consequences to the Theory of Polarization
 - BB. Diffusion Equations for Rotation and Translation
 - 1. The Problem of Analytical Tractability
 - 2. The Problem of Over-Parameterization
- V. Symmetry
- A. Parity Inversion
 - B. Time Reversal
 - C. Application to Time-Correlation Functions
 - D. The Application of Group Theory to Time-Correlation Functions
 - E. Point-Group Theory in Frame (X, Y, Z)
 - F. Frame (x, y, z) Molecular Point-Group Theory
 - G. Ensemble Averages of Scalars
 - H. Ensemble Averages of Vectors
 - I. Ensemble Averages of Tensors
 - J. Ensemble Average Properties in Frame (x, y, z) —Some Examples
 - K. Higher-Order Tensors
 - L. The Effect of External Fields
 - M. Fundamental Dynamics: The Noninertial Frame of Reference
 - N. Consequences for the Theory of Diffusion
 - O. A Simple Langevin Theory of ccf's in Frame (X, Y, Z)
 - P. The Role of the Intermolecular Potential

- Q. Patterns of Cross Correlations in Frames (X, Y, Z) and (x, y, z)
- R. The Omega Pattern in Frame (x, y, z)
- S. The \hat{D}_f Pattern in Frame (X, Y, Z)
- T. Other Patterns in Frame (X, Y, Z)
- U. Symmetry of Some ccf's
- V. Analytical Theory of Field-Induced ccf's
- VI. Time-Cross Correlation Functions—A Major Challenge to Diffusion Theory
 - A. Ccf's Involving Molecular Vibration
 - B. Computer Simulation of Flexible Water
 - C. The Effect of Internal Vibrations on Correlation Functions
 - D. Cross-Correlation Functions
 - E. Vibration-Translation
 - F. Rotation-Translation
 - G. Simulation Results for Water from 10 to 1273 K
 - H. Time ccf's from 10 to 1273 K
 - I. Higher-Order ccf's
 - J. Solutions of Water in Carbon Tetrachloride
 - K. Liquids of Spherical Top Molecules
 - L. The Effect of External Fields in Liquid Water
 - M. Circularly Polarized Laser Field
 - N. Chiral Liquids
 - O. Circular Flow in Liquid Water
 - P. Other Types of Applied External Field
 - Q. Removal of H-Bonding—The Computer Simulation of Hydrogen Selenide
 - R. Some Consequence for Quantum Mechanics
 - S. Analogies between Quantum and Classical Mechanics
 - T. Rod-like Molecules and Liquid Crystals
 - U. Survey of Results and Future Progress
- VII. Group Theory and Statistical Mechanics
 - A. Point-Group Theory in Frame (X, Y, Z)
 - B. The First Principle (Neumann-Curie Principle)
 - C. D Representations in Frame (X, Y, Z)
 - D. Point-Group Theory in Frame (x, y, z)
 - 1. Principle 2
 - E. The Effects of Fields—Principle 3
 - 1. Principle 3
 - F. Symmetries in Frame (x, y, z)
 - G. External Fields: Symmetries
 - H. The Weissenberg Effect
 - I. Chirality
 - J. Nonequilibrium: New Fluctuation Dissipation Theorems
 - K. Application of the Theorem to Dielectric Relaxation and the Dynamic Kerr Effect
 - L. Experimental Observations
 - M. New Dichroic Effects and Absolute Asymmetric Synthesis
 - N. Spin-Chiral and other Dichroic Effects from Principle 3
 - O. Symmetry Effects in Liquid Crystals
 - P. Basic Symmetry Arguments in Nematogens and Cholesterics
 - 1. The $C_{\infty h}$ Swarm

- 2. The $D_{\infty h}$ Swarm
- 3. The C_{∞} Swarm
- 4. The D_{∞} Swarm
- 5. The Electrically Aligned Nematogen
- 6. The $C_{\infty v}$ Nematogen
- 7. The $D_{\infty h}$ Nematogen
- 8. The C_{∞} Cholesteric
- 9. The D_{∞} Cholesteric
- Q. The Effect of a Shearing Field
- R. Computer Simulation—A Specific Application
- S. Symmetry in Smectic Liquid Crystals
 - 1. Local Smectic Point Groups
 - 2. Mapping from $R_h(3)$ to the Smectic Point Groups
- T. Time-Reversal Symmetry
- VIII. Simulation and Symmetry in Non-Newtonian Fluid Dynamics
 - A. Representation of Simple Couette Flow
 - B. Consequences for Langevin Theory
 - C. Derivation and Solution of the Langevin Equations
 - D. Shear-Induced Structural Effects and gtsm
 - E. Crystal-Like Arrested States at High Shear Rates—An Excess of Symmetry
 - F. Hexagonal C_{3h} (Hermann Mauguin $\bar{6}$)
 - G. Shear-Induced Depolarized Light Scattering
 - H. Light-Scattering Geometry
 - I. Polarimetry
 - K. Shear Symmetry in the Dielectric and Far Infrared
 - L. Shear-Induced Molecular Polarizability and Polarization
 - M. Adaptation of the Morriss-Evans Theorem
 - N. Shear-Induced Dipole Relaxation and Far Infrared Power Absorption
 - O. The D Symmetries of Shear in the Presence of Fields
- IX. New Pump-Probe Laser Spectroscopies: Symmetry and Application to Atomic and Molecular Systems
 - A. Basic Symmetry Concepts
 - B. Complete Experiment Symmetry
 - 1. Wigner's Principle of Reversality (T)
 - 2. Wigner's Principle of Parity Inversion (P)
 - C. The Symmetry of Cause and Effect: Group Theoretical Statistical Mechanics
 - D. The D Symmetries of Natural and Magnetic Optical Activity
 - E. Application of gtsm—Combined Field Symmetries
 - F. Application of gtsm to Nonlinear Optical Activity
 - G. Optical Activity Induced by a Pump Laser
 - H. Some Expected Π -Induced Spectroscopic Effects
 - I. Π -Induced Zeeman Splitting
 - J. Rayleigh-Raman Optical Activity Induced by Π
 - K. Forward-Backward Birefringence due to Π
 - L. Parity Violation in Molecular Ensembles due to Π
 - M. The Optical Zeeman Effect—Quantization of the Imaginary Part of the Atomic or Molecular Polarizability (the Electronic Orbital-Spin Angular Polarizability)

- N. Semiclassical Theory of the Optical Zeeman Effect
- O. Laser-Induced Electronic and Nuclear Spin Resonance
- P. Rayleigh-Raman Light-Scattering Optical Activity due to Optical Rectification
- Q. Forward-Backward Birefringence due to Optical Rectification
- R. The Optical Faraday Effect—Order-or-Magnitude Estimate of the Angle of Rotation of a Plane-Polarized Probe
- S. Electric Circular Birefringence and Dichroism
- T. Frequency-Dependent Electric Polarization due to Optical Rectification in Chiral Ensembles
- U. Symmetry of Laser-Induced Electric Polarization in Chiral Single Crystals
- V. Electrodynamics of a Rotating Body—Some Spectral Consequences of the Lorentz Transformation
- W. Parity Nonconservation in New Laser Spectroscopies

Acknowledgments

References

Appendix: Molecular Dynamics Simulation Algorithm "Tetra"

INTRODUCTION

This chapter deals with the impact of contemporary computer simulation on our understanding of molecular diffusion processes. It argues the case for the classical equations of motion applied to the minute time scales and dimensions of molecular dynamics. It is therefore assumed implicitly, as is the contemporary practice, that classical mechanics is valid in this context, although there is no rigorous proof of why this should be so. The traditional approach to the theory of molecular diffusion, developed at the turn of the century, does not stand up to the data now available. These are obtained contemporaneously from many spectral sources, and from computer simulation using increasingly powerful techniques. These data now show unequivocally that the traditional approach is fundamentally flawed in at least one respect, the assumption that translational and rotational motion are decorrelated. We now have available a set of nonvanishing time-cross correlation functions with which to define and elaborate upon the fundamental physical properties of molecules diffusing in three dimensions.

The chapter is intended to be readily understandable to undergraduates and also to be useful to specialists in molecular diffusion, computer simulation, and several branches of spectroscopy. It opens with a description of the traditional theory, whose mathematical complexity is kept secondary to the essentially simple physical concepts that make up the Langevin equation of diffusion. Einstein's theory of translational Brownian motion, which was used to prove the existence of molecules, and Debye's theory of rotational diffusion, which was used to prove the molecular

origin of the dispersion of dielectric permittivity at radio frequencies, are discussed in terms of simple Langevin equations, whose limitations are clearly defined. These include the failure to describe the far infrared (high frequency) part of the dispersion of permittivity and dielectric loss in dipolar molecular liquids, due to a missing inertial term and inadequate description of the intermolecular potential energy. The relation of the Langevin to the Liouville equation shows that the former is a first approximation to the trajectory of a diffusing asymmetric top in a three-dimensional ensemble of similar molecules. The experimental consequences of this approximation are most visible in the far infrared, but also in other types of data, discussed in Section II.

This section makes a survey of the available spectral data on molecular diffusion, and compares the results for consistency from sources such as combined dielectric and far infrared spectroscopy, the relaxation of nuclear magnetic resonance, light scattering, infrared band shape analysis, Raman scattering, ultra and hyper sound relaxation, and inelastic, incoherent, neutron scattering. Correlation times for one test liquid, dichloromethane, are compared from all spectral sources and with their equivalents from computer simulation. The latter brings some self consistency into what remains an imperfect experimental understanding due to inadequate data coverage.

Section III covers the basics of computer simulation with reference to the numerical integration of the classical rotational and translational equations of motion of the three dimensional diffusion of the asymmetric top molecule dichloromethane in the liquid state. This section covers the approximation of the intermolecular potential with the pairwise additive method, the computation of thermodynamic properties, and spectral data, from the individual trajectories of the simulation.

In Section IV some new results from computer simulation are described, and limits set on the validity of traditional linear response theory. These are described in terms of new effects discovered by the simulation technique, such as fall transient acceleration and field decoupling. The importance of cross-correlation functions is illustrated with respect to the effect of external force fields that are shown by simulation to induce such previously unknown correlations direct in the laboratory frame of reference (X, Y, Z).

Section V introduces the use of symmetry laws that govern the existence of cross-correlation functions both in frame (X, Y, Z) and in frame (x, y, z) fixed in the molecule as it diffuses. These include parity and time-reversal symmetry, and group theory in both frames. Tables are provided to guide the reader as to the use of group theory in the context of time correlation functions of all orders, and for representative molecular point groups.

Some theories of the time dependence of members of the set of cross-correlation functions are described briefly in order to illustrate the limits of validity of the traditional approach of Section I.

Section VI describes the challenge to diffusion theory of the existence of many members of this set for all molecular matter. The nature of the set of cross-correlation functions is illustrated with reference to water under a broad range of conditions, with respect to correlations involving simultaneously vibration, rotation, and center of mass translation in a liquid, with respect to rod-like molecules as models for liquid crystal behavior, and to highly anisotropic diffusers in the liquid state. Some indications are given to the meaning of cross-correlation functions in the context of quantum mechanics, where they become expectation values of wave functions involving both rotational and translational energy levels. The conditions are described under which the rototranslational spectral features corresponding to these energy levels may be observed by spectroscopy.

Section VII introduces group theoretical statistical mechanics, and gives the three principles which govern the application of group theory to the process of molecular diffusion. These principles are illustrated with respect to both frames (X, Y, Z) and (x, y, z) in molecular liquids and liquid crystals.

Section VIII extends the scope of group theoretical statistical mechanics to the effect of fields of various kinds on molecular liquids, and introduces the study of non-Newtonian rheology with the principles of group theory. These chapters are filled out with reference tabular material and illustrations which should be useful for a broad cross section of chemical and computational physicists and flow engineers.

Finally, Section IX deals with the symmetry and simulation of new pump-probe spectroscopies, utilizing the principles outlined in Sections VII and VIII.

I. THE TRADITIONAL VIEW

The traditional approach to molecular diffusion in liquids is a first approximation to the problem of dealing with a very large number of moving and interacting molecules.¹⁻⁴ Conventional textbooks⁵⁻¹⁵ tend to overemphasise the applicability of the turn of the century techniques first used to deal with this problem. Albert Einstein was the first to realize, in a Berne patent office at the dawning of modern physics, that the restless motion of pollen particles known as *Brownian motion* was caused by unending collisions with much smaller particles, and these he recognised as molecules. Their dynamical trajectories, he assumed, were governed by classi-

cal statistical mechanics. In a paper published in 1905, Einstein¹⁶ estimated the Avogadro Number from a diffusion equation developed to explain the Brownian motion on the basis of molecular collisions with the much heavier and slower moving pollen particles, whose motion could be studied directly through a microscope. This paper provided one of the first definitive proofs of the existence of molecules as the fundamental entities of molecular matter.

Einstein measured his limits, he did not, for example, take into account the rotational motion of each molecule because this was not needed for the estimation of the Avogadro Number from the observation of Brownian motion. He based his theory on well-defined assumptions, and developed it self-consistently. Now, almost a century later we are privileged to have available a vast ocean of data from computer simulation⁴ and far infrared spectroscopy,¹ for example, which describe in abundant detail worlds which the pioneer could but dimly perceive. Our understanding of molecular diffusion has been transfigured in the last 20 years.

This chapter attempts to review the significant results of the last decade or so and to reassess critically the early theories of molecular diffusion¹⁶⁻¹⁹ with new data. The chapter argues the case, for the time being, for a classical mechanical approach to the dynamics of molecular liquids, using the Newton and Euler equations, and variations. This is made possible by contemporary supercomputers. There are fewer approximations than in the traditional theory of diffusion, and the new methods are well founded in the laws of classical physics.

A. Einstein's Theory of Translational Brownian Motion

The explanation for Brownian motion given by Einstein¹⁶ makes several assumptions about the nature of the collision between a pollen particle and a molecule of the surrounding liquid. The basic idea is that the effect of collisions produces random jumps in the position of the pollen particle. The velocity change on collision is assumed to be damped out quickly and the role of velocity in Einstein's treatment is ill-defined.^{7,20} The random walk of the pollen particle in three dimensions is described by a partial differential equation for the displacement in each dimension. The solution of this equation showed that the mean-square displacement of a Brownian particle should increase linearly with time. This prediction was verified experimentally by Perrin²¹ in 1908, and from Einstein's formula a value of Avogadro's Number was deduced which is in satisfactory agreement with the accepted value.

A contemporary description of the methods used by Einstein to derive the formula for the mean-square displacement of the pollen particle is given by W. T. Coffey in Ref. 4. A straightforward description of the

reasoning behind the theory was established by Langevin¹⁷ in 1908. This is more transparent to the student of Brownian motion, and also reveals more clearly the limitations of the methods involved in calculating both the mean-square displacement and the Avogadro Number.¹⁻⁴

B. The Langevin Equation for Translational Brownian Motion

Langevin's treatment is limited to the motion of large pollen particles in suspension in a molecular environment. The equation has often been applied uncritically, however, to the motion of a molecule in solution in others. There are fundamental differences in the nature of a collision between two molecules and between a molecule and pollen particle. The transfer of momentum in the former case is roughly equally shared, and the assumption that the change in velocity can be ignored does not hold. This was realized fully as late as 1964, following a computer simulation by Rahman²² of 864 diffusing argon atoms. In this simulation, the velocity auto correlation function of the ensemble of argon atoms was found to be markedly different in time dependence from the simple exponential of early diffusion theory, based on the Einstein theory of translational Brownian motion.

Langevin wrote the equation of translational Brownian motion as

$$m \frac{d^2x(t)}{dt^2} + m\beta_T \frac{dx(t)}{dt} = F(t) \quad (1)$$

assuming that the forces on the pollen particle could be divided into a systematic part $-m\beta_T \dot{x}(t)$, representing a friction on the pollen particle generated by its molecular collisions, and a random force $F(t)$ generated by a random walk of the position of the pollen particle relative to the surrounding molecules. The frictional force opposes the motion and is therefore given a negative sign, and the random force generates the unending motion of the pollen by collision with molecules which are in constant thermal motion and have constant kinetic energy at constant temperature. Langevin assumed that the frictional term was governed by Stokes's law of macroscopic hydrodynamics, which applies to a spherical particle in a viscous fluid. In contrast, the random force $F(t)$ was assumed to be independent of x and to vary very rapidly compared with any variation in $x(t)$. There is no *statistical correlation* between $F(t)$ and $F(t + \Delta t)$. The picture is therefore a mixture of hydrodynamic and statistical concepts. It has fundamental mathematical limits as described by Doob.²⁰ Its physical shortcomings were not easily found until the computer simulation by Rahman, using the much older Newton equations of motion. The Lange-

vin equation is really an ad hoc mixture of concepts. In the same way, Einstein's estimate of the Avogadro Number was based on a combination of his result for the mean square displacement

$$\langle \Delta x^2 \rangle = \frac{kTt}{3\pi\eta a} \quad (2)$$

with Stokes's Law for the friction coefficient

$$\beta_T = 6\pi\eta a \quad (3)$$

Here a is the effective radius of the pollen particle, assumed spherical, η is the effective viscosity of the molecular surroundings, and t is the time after an arbitrary initial instant for which the particle has been under the influence of the Brownian random walk. There was no rigorous justification for the mixture of concepts, except that it seemed to work at first, providing a good approximation to the Avogadro Number.

This early work was, however, pivotal, because it was the first to use the concept of molecular dynamics in explaining Brownian motion. It provided evidence for the existence of molecules when such evidence was needed. The role of contemporary computer simulation is very different.

C. Contemporary Criticisms of the Traditional Approach

One of the most powerful arguments against the indiscriminate use of the Langevin equation is that it cannot be derived rigorously from the fundamental equations of motion used in statistical mechanics, for example the Liouville equation. This was demonstrated clearly by Mori²³ in 1965, using projection operators. Mori started from the Liouville equation

$$\dot{\Gamma} = iL\Gamma \quad (4)$$

where L is the Liouville operator and Γ is the phase space of positions and momenta. Mori showed that a dynamical quantity A or \mathbf{A} (i.e., scalar or vector) which obeys the Liouville equation

$$\dot{A} = iLA \quad (5)$$

also obeys the equation

$$\dot{A} = i\Omega_A A(t) - \int_0^t \phi_A(t-\tau) A(\tau) d\tau + F_A(t) \quad (6)$$

which is the same equation as (5). Here Ω_A is the resonance operator, and ϕ_A is the *memory function*. F_A is a vector of random quantities. Equation (6) reduces to the Langevin equation only when the resonance operator vanishes and when the memory function is a delta function of time. If A represents linear velocity, v for example, the original Langevin equation (1) is recovered only with these drastic approximations. *The memory function can never be a delta function for any meaningful molecular dynamical process.* Mori showed that repeated application of projection operators to the Liouville equation produces a string of interrelated equations of the type (6), but never a simple Langevin equation of type (1). Laplace transformation of the string of equations produces the *Mori continued fraction*¹⁻³ for the statistical correlation between the variable A at time t and its value at $t = 0$, the *velocity autocorrelation function*. The equivalent result from the simple Langevin equation is an exponential in time, an oversimplification of the rigorous Mori continued fraction. Rahman's computer simulation of 1964²² showed conclusively that the velocity autocorrelation function was far from being a simple exponential in 864 argon atoms interacting with a realistic (Lennard Jones) model for the interatomic potential.

D. Molecular Translation and Rotation

By restricting consideration to spherical particles the treatment so far has not begun to account for rotation, and for simultaneous rotation and translation in an irregular body, or "asymmetric top," diffusing in three dimensional space (X, Y, Z). The dispersion of the dielectric permittivity at radio frequencies was known in the first decade of this century to be a rotational phenomenon involving the molecular antenna, the permanent molecular dipole moment, μ . In general this rotation occurs on top of the translation in three dimensions. There is a statistical spread of angular velocities which causes the dielectric permittivity of a molecular liquid to be frequency dependent.¹⁻⁴ The dipole moment is the result of an asymmetric distribution of charge, due to the distribution of atoms within a molecule. The dispersion of permittivity is always accompanied by a dielectric loss as the frequency of the measuring field is increased. This is governed by a relatively slow motion, the rotation of the whole molecule, and can be observed using conductance/capacitance changes, or by the direct attenuation of radiation, at *far infrared* frequencies.^{12,24} The interaction of molecular (and other) matter with electromagnetic radiation is governed by electromagnetic field theory, based classically on Maxwell's equations.

E. Dielectric Relaxation and the Debye Theory of Rotational Diffusion

Essentially speaking, dielectric relaxation involves the partial polarization⁹⁻¹⁴ of the molecules of a liquid with an electric field. If this alternates in frequency, the periodic change in direction produces a change in direction of the molecular dipole moments as the molecules attempt to rotate and follow the field direction. The electric field produces only a very slight alignment of the molecules, because the thermal motion is relatively so much more energetic at room temperatures and available electric field strengths. The degree of alignment is governed essentially by the ratio

$$b = \frac{\mu E}{kT} \quad (7)$$

where E is the electric field, k the Boltzmann constant, and T the temperature in absolute units. The ratio b is the argument of the Langevin function, measuring the degree of alignment produced by the external field, the result of competition between the aligning energy and the thermal energy, kT .

F. Loss of Polarization

The simplest kind of dielectric relaxation occurs when a static electric field is applied initially to a liquid of diffusing molecules, allowing enough time for alignment to occur, and is then switched off instantaneously. The degree of molecular alignment produced by the external electric field is lost, but not immediately. The natural thermal motion that makes alignment a difficult process also prevents its instantaneous loss. The length of time needed to align the sample as fully as possible by an applied static electric field, and conversely, the time needed for loss of alignment, both depend on the nature of molecular diffusion. This fact can be used experimentally¹² to investigate the nature of diffusion. In the alignment process, the degree of orientation of the molecules as a function of time is known as the rise transient, and the loss of alignment as the fall transient. These can only be calculated theoretically by a full consideration of the molecular dynamics. In particular, the rotational dynamics of each molecule in its molecular environment must be known in detail, because the rise and fall transients are both products of the rotational torque generated by the vector product of the electric field and the molecular dipole moment. No progress at all can be made, therefore, with theories of translational diffusion.

G. The Concept of Rotational Diffusion

Debye was the first to develop a theory¹⁹ of *rotational diffusion*. This was first applied to explain a form of dielectric relaxation which led to a decrease in relative permittivity with the increasing frequency of an applied, alternating, electric field. This had been observed to occur in dipolar molecules whose charge distribution was not symmetrical. The phenomenon could therefore be used to investigate the structure of molecules. Debye reduced the problem⁵ to considering the two dimensional Brownian motion of a dipole in an external, time-varying electric field. The original approach^{5,19} is summarised in Ref. 4 and involved the use of a Smoluchowski equation¹⁸ with the x coordinate of translational diffusion replaced by the angular coordinate θ . The Langevin equation for Debye's two dimensional rotational diffusion theory is

$$\beta_R \dot{\theta}(t) + \frac{\partial V(\theta, t)}{\partial \theta} = \lambda(t) \quad (8)$$

where λ is the random torque from the Brownian movement of the surroundings, and β_R is the rotational friction coefficient. The potential energy due to the aligning field is

$$V = -\mu E \cos \theta = -\boldsymbol{\mu} \cdot \mathbf{E} \quad (9)$$

We can see immediately from a comparison of the rotational Langevin equation (8) used by Debye⁵ and the translational Langevin equation (1) that there is a term missing in the former, that is, $I\dot{\theta}(t)$, the inertial term. The rotational equation ignores from the outset the finite rotational acceleration of each diffusing molecule. Einstein also effectively ignored the inertial term in arriving at his value of the diffusion coefficient, (Ref. 4, pp. 86 to 87).

H. Rise Transient

The solution of the Langevin equation (8) for the alignment of the molecular dipole moments by an applied static electric field is the mirror image of its solution (the fall transient) after the instantaneous removal of the field. To compute the rise transient we merely solve the Langevin equation for the fall transient, which is Eqn. (8) with

$$V = 0 \quad (10)$$

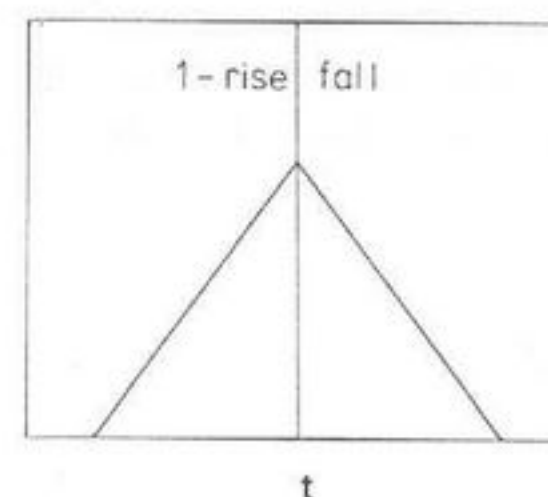


Figure 1. Log of rise and fall transients in Debye's theory of rotational diffusion. One is an exponential increase in molecular orientation and the other a mirror image decrease (schematic).

I. The Fall Transient

This is obtained from the Langevin equation as

$$\langle \cos \theta \rangle = \frac{\mu E}{2kT} e^{-t/\tau_D} \quad (11)$$

where τ_D is the Debye relaxation time. The fall and rise transients in the Debye theory of rotational diffusion are therefore both exponentials in time, one the mirror image of the other as sketched in Fig. 1.

J. Polarization and Frequency Spectrum

The polarization decay after the instantaneous removal of the aligning electric field is therefore a simple exponential in this approximation. If we reinstate the missing inertial term, however, the polarization decay becomes^{25,26}

$$\langle \cos \theta \rangle = \frac{\mu E}{kT} \exp \left\{ -\frac{kTI}{\beta_R^2} \left(\frac{\beta_R t}{I} - 1 + e^{-\beta_R t/I} \right) \right\} \quad (12)$$

where I is the molecular moment of inertia. Equation (12) reduces to Eq. (11) only at very long times, that is, as t goes to infinity. This immediately shows that the Debye rotational diffusion theory, and the model upon which it is based, Eq. (1) with its inertial term missing, work only over relatively long time scales or low frequencies. They are "coarse grained" theories of molecular diffusion and dynamical evolution. Something goes wrong in both theories as the time scale of events becomes shorter and shorter.

To realize these shortcomings is a necessary step towards progress in the theory of molecular diffusion. Short time scales mean high frequencies, long time scales low frequencies conversely. In mathematical terms there is always a rigorous and general relation between a given function of time

which is continuous and differentiable in the range of interest and its counterpart in frequency, known as the *frequency spectrum*. This is the Fourier Integral Theorem, which may be written as

$$C(\omega) = \frac{1}{2\pi} \int_{-\infty}^{\infty} C(t) e^{-i\omega t} dt \quad (13)$$

$$C(t) = \int_{-\infty}^{\infty} C(\omega) e^{i\omega t} d\omega \quad (14)$$

Here ω is the angular frequency in radians per second, and if $C(\omega)$ is an angular frequency spectrum, then $C(t)$ is a correlation function.¹ There are many types of correlation function available from modern spectroscopy^{1,4} and so there are many types of time correlation. In statistics, "correlation" is the interdependence of quantitative data. The time correlation function is in general the product of two dynamical variables averaged in a special way. It is the internal correlation between two observations in time. The normalized autocorrelation function can be defined in general as

$$C(t) = \lim_{T \rightarrow \infty} \left\{ \frac{\int_0^T (1/T) A(t) A(t + \tau) dt}{\int_0^T A^2(t) dt} \right\} \quad (15)$$

The numerator is the autocovariance, the denominator is the variance, and this type of average is called the running time average. By a basic theorem of statistics¹ it is rigorously equivalent to the Maxwell-Boltzmann ensemble average for a stationary ensemble at reversible thermodynamic equilibrium. The autocorrelation function (acf) of the molecular dipole moment μ is the Fourier transform of the complex dielectric permittivity. The power absorption coefficient of the high frequency far infrared is the Fourier transform¹ of the autocorrelation function of the second time derivative of $\langle \mu(t) \mu(0) \rangle$.

This is known as the rotational velocity acf. Furthermore, the power absorption coefficient of the far infrared, $\alpha(\bar{\nu})$, in neper per cm, is related fundamentally to the dimensionless dielectric loss $[\epsilon(\omega)]$ through Maxwell's equations

$$\alpha(\omega) = \frac{\omega \epsilon''(\omega)}{n(\omega)c} \quad (16)$$

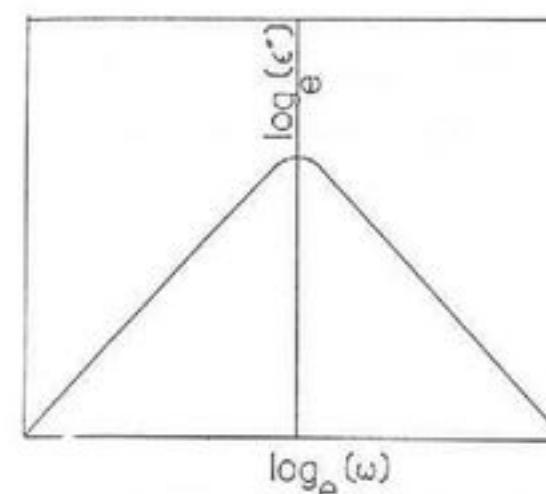


Figure 2. A plot of dielectric loss against the logarithm of frequency. In Debye's theory, this is the well-known bell-shaped curve of dielectric relaxation theory (schematic).

where $n(\omega)$ is the refractive index of the liquid at far infrared frequencies and c is the velocity of light.

There is a chain of relations between the frequency-dependent complex dielectric permittivity

$$\epsilon = \epsilon'(\omega) - i\epsilon''(\omega)$$

the far infrared power absorption coefficient and the acf.'s of the molecular dipole moment and its derivative.

K. Dielectric and Far Infrared Spectrum

Dielectric spectra, the frequency dependence of the dielectric loss,^{12,24} and far infrared spectra, that of the power absorption coefficient, are obtained at low frequencies and high, respectively. Although they are observed with entirely different experimental methods, they are always interrelated by Eq. (16). It is obvious that the theory of rotational diffusion of Debye must produce a self-consistent picture of both spectra, which can stretch over a vast frequency range.^{1,4,12} This is clear in hindsight, but for over half a century the definitive experimental test of fundamental molecular diffusion theory was delayed by lack of high-frequency data and misunderstandings due to the missing inertial term. The Debye theory seemed to produce results in excellent agreement¹⁴ with the observed angular frequency dependence of complex permittivity at low frequencies, where the well-known bell shaped curve^{12,14,24} appears to be the single dominant feature (Fig. 2). This is the Fourier transform of an exponential function of time. According to a theorem of linear response theory,¹⁻⁴ known as the fluctuation-dissipation theorem, the fall transient of Eq. (11) has the same time dependence as the acf of the molecular dipole moment

$$\frac{\langle \mu(t) \cdot \mu(0) \rangle}{\langle \mu^2 \rangle} = \frac{\langle \cos \theta \rangle}{\langle \cos \theta(0) \rangle} \quad (17)$$

when both are normalized to the value of 1 at $t = 0$. The Debye theory of rotational diffusion therefore produces an exponential normalized orientational acf

$$C_{\mu}(t) = \frac{\langle \boldsymbol{\mu}(t) \cdot \boldsymbol{\mu}(0) \rangle}{\langle \mu^2 \rangle} = e^{-t/\tau_D} \quad (18)$$

where τ_D is the Debye relaxation time. The contemporary theory of statistical mechanics shows that the frequency dependence of the dielectric loss²⁷ and dispersion is obtained by Fourier transformation of the orientational acf. The well-known bell-shaped curve obtained by Debye is the result of an exponential fall transient, whose time dependence has been taken to be the same as that of the orientational acf at equilibrium. By a comparison of the results of the original Debye theory (Eq. 11) and the same theory corrected for its missing inertial term (Eq. 12) we have seen that the original theory can be valid only at low frequencies. At the time the Debye theory was developed, and for 50 years thereafter, only low-frequency data were available to test the theory. Its apparent success in explaining these data masked its inherent flaws. The theory became accepted uncritically.^{9,14}

L. The Debye Plateau

If we neglect the complications of the internal field effect, that is, the difference between the applied electric field and that actually felt by a diffusing molecule at an instant in time, the relation between dielectric loss and the normalized orientational acf $C_{\mu}(t)$ can be shown¹ to be the following, which are valid in dilute solutions of dipolar molecules in other, symmetrical, (nondipolar) molecules such as carbon tetrachloride or sulphur hexafluoride:

$$\epsilon''(\omega) = \frac{N\mu^2\omega}{3kT\epsilon_0} \int_0^{\infty} C_{\mu}(t) \cos \omega t dt \quad (19)$$

$$\alpha(\omega) = \frac{N\mu^2\omega^2}{3kT\epsilon_0 c} \int_0^{\infty} C_{\mu}(t) \cos \omega t dt \quad (20)$$

$$C_{\mu}(t) = \frac{2}{\pi} \frac{3kT\epsilon_0 c}{N\mu^2} \int_0^{\infty} \frac{\alpha(\omega)}{\omega^2} \cos \omega t d\omega \quad (21)$$

Here ϵ_0 is the dielectric permittivity at static frequencies, N is the molecular number density (the number of molecules per unit volume), and $\alpha(\omega)$ is the far infrared power absorption coefficient in neper cm^{-1} . From Eqs.

(18) and (19) the result is obtained that the dielectric loss corresponding to an exponential dipole acf is, in dilute solution

$$\epsilon''(\omega) = \frac{N\mu^2}{3kT\epsilon_0} \frac{\omega\tau_D}{1 + \omega^2\tau_D^2} \quad (22)$$

Combining this equation with (16) it can be seen that the infrared power absorption coefficient from Debye's rotational diffusion theory is

$$\alpha(\omega) = \frac{N\mu^2}{3kT\epsilon_0 n(\omega)c} \frac{\omega^2\tau_D}{1 + \omega^2\tau_D^2} \quad (23)$$

This is well behaved at low frequencies and vanishes with the angular frequency, but at high frequency leads to the Debye plateau¹²

$$\alpha(\omega) \xrightarrow{\omega \rightarrow \infty} \frac{N\mu^2}{3kT\epsilon_0 n(\omega)\tau_D c} \quad (24)$$

In Debye's diffusion theory all molecular dipolar liquids must be opaque at all frequencies from the far infrared upwards, including the visible, an absurd result.

M. Far Infrared Interferometry

The development of computers gave great impetus^{1,28,29} to the exploration of the far infrared region by Fourier transformation of interferograms obtained by Michelson interferometry. This optical technique produces patterns of light intensity from two interfering beams of far infrared radiation as a function of distance travelled by a mirror in one arm of a Michelson interferometer. The radiation reaching a heat-sensitive Golay detector is recorded as the mirror travels and is known as an interferogram. Fourier transformation of the interferogram (a type of correlation function in distance) produces the far infrared spectrum. Fourier transform spectroscopy now dominates infrared and NMR spectroscopy.

In the late 1960s, about 60 years after Debye proposed his theory of rotational diffusion, it became possible to explore the behavior of molecular liquids at frequencies in the far infrared, which stretches from the upper end of the gigahertz range (microwave) and beyond into the infra-

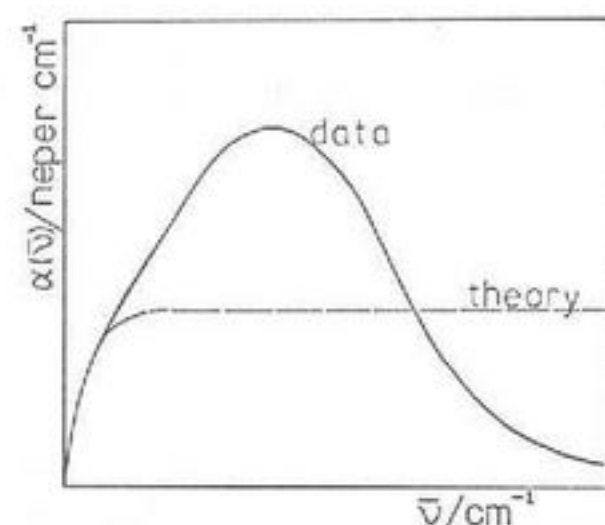


Figure 3. Far infrared power absorption coefficient of liquid dichloromethane at room temperature (solid line) compared with the theoretical prediction of Debye type rotational diffusion (dashed line).

red. Figure 3 illustrates that the far infrared absorption of a dipolar molecular liquid such as dichloromethane¹ in the range from about 2 cm^{-1} to about 250 cm^{-1} greatly exceeds in intensity of power absorption the Debye plateau computed for that liquid. At very high frequencies the power absorption coefficient once more reaches zero, that is, drops away from the Debye plateau. There is little or no resemblance at these frequencies between theory and experiment.

If however, we compare the same set of data and the same theory in terms of dielectric loss, over the same frequency range, using Eq. (16) to convert the power absorption coefficient to dielectric loss, the result is a deceptively good fit of theory and data, Fig. 4. The theory of rotational diffusion seems to perform well at low frequencies when expressed in terms of dielectric loss, but fails completely at high frequencies when expressed in terms of the far infrared power absorption coefficient in neper per centimeter.

N. The Effect of Including the Inertial Term in Eq. (8)

The procedure of including the inertial term in the rotational Langevin equation used by Debye, Eq. (8), is known as the "inertial correction"

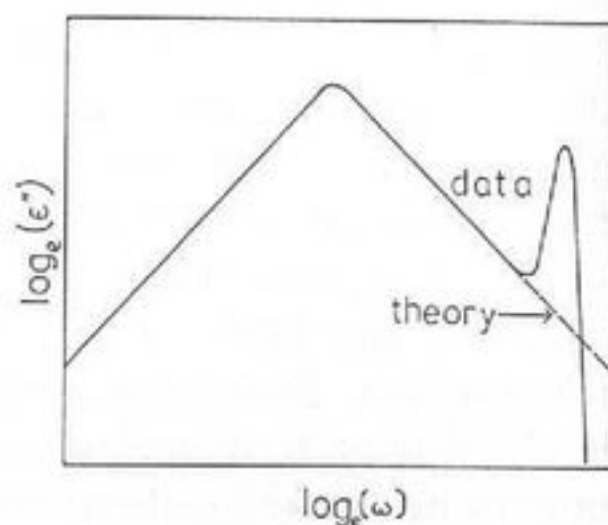


Figure 4. The comparison illustrated in Fig. 3 made in terms of the dielectric loss at lower frequencies than the far infrared (schematic).

to the Debye theory of rotational diffusion. The spectrum in the dielectric and far infrared frequency regions obtained from the inertia-corrected Debye theory is the Fourier transform of the correlation function

$$C_{\mu}(t) = \frac{\langle \mu(t) \cdot \mu(0) \rangle}{\langle \mu^2 \rangle} = \exp \left\{ -\frac{kTI}{\beta_R} \left(\frac{\beta_R t}{I} - 1 + e^{-\beta_R t/I} \right) \right\} \quad (25)$$

This can be expressed in terms of the continued fraction

$$\frac{\alpha_p(\omega)}{\alpha_p'(0)} = 1 - \frac{i\omega/\beta}{i\omega/\beta + \frac{\gamma}{1 + i\omega/\beta + 2\frac{\gamma}{2 + i\omega/\beta + 3\gamma \dots}}} \quad (26)$$

where $\alpha_p(\omega)/\alpha_p'(0)$ is the normalized polarizability. This expression was first obtained by Sack²⁵ from the probability diffusion equation corresponding to the Langevin equation

$$I\ddot{\theta}(t) + \beta_R \dot{\theta}(t) = \lambda(t) \quad (27)$$

Here γ is $kT/I\beta^2$; with

$$\tau_D = \frac{\beta_R}{kT} = \frac{I\beta}{kT}; \quad \beta = \beta_R/I \quad (28)$$

The original Debye rotational diffusion theory is equivalent to the first convergent³ of this continued fraction, that is,

$$\frac{\alpha_p(\omega)}{\alpha_p'(0)} = \frac{1}{1 + i\omega\tau_D} \quad (29)$$

with

$$\tau_D = \frac{\beta_R}{kT}$$

The second convergent gives Rocard's equation

$$\frac{\alpha_p(\omega)}{\alpha_p'(0)} = \frac{1}{1 + i\omega\tau_D - \omega^2\tau_D/\beta} \quad (30)$$

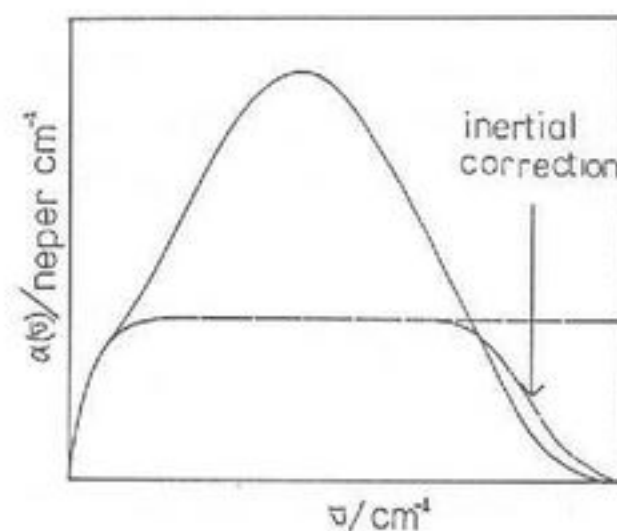


Figure 5. The effect of correcting Debye's theory for the missing inertial term.

which was the earliest attempt (1933) to correct the Debye theory for the missing inertial term. Rocard produced Eq. (30) from a Smoluchowski diffusion equation in which he replaced the term left out by Debye in 1913.

However, the only effect on the theoretical power absorption coefficient in the far infrared of taking any convergent of Sack's continued fraction is to produce a high-frequency return to transparency from the Debye plateau. The inertia-corrected Debye theory fails^{25,26} to describe the observed far infrared power absorption coefficient, as illustrated in Fig. 5.

O. Rotational Diffusion in a Potential Well: The Itinerant Oscillator

There is something more fundamental lacking in the simple theory of rotational diffusion than a missing inertial term. The unrealistic nature of the rotational Langevin equation (8) when used to describe data from molecular diffusion is exposed starkly by a result such as that of Fig. 5. Several approaches have been devised²⁴ to meet this fundamental difficulty, sharing the common feature that the diffusion of an individual molecule was for the first time described theoretically as a process involving torsional oscillation or libration^{12,29} with an ever-changing cage of nearest-neighboring molecules. Essentially, the featureless environment of the friction term in Langevin's own treatment was given some shape. It was recognized that a diffusing molecule must simultaneously undergo oscillatory motion of the diffusing center of mass, combined with torsional oscillation about this point in the laboratory frame (X, Y, Z). The influence of Langevin and his contemporaries was so overwhelming, however, that the new approach to diffusion theory which slowly emerged during these years tied itself to the pioneering concept of the Langevin equation, and the equivalent equations for the evolution of probability density developed¹⁻⁴ by Smoluchowski, Fokker, Planck, Klein, and Kramers. The new approach still stuck to the concept of rotational diffusion, and left translation out of consideration.

As we shall see, this turns out to be the only tractable way of extending the validity of rotational diffusion, the only way which avoids a morass of mathematical complexity dealing with too many unknown (empirical) parameters. We perceive for the first time very general and profound limitations on the concepts devised at the turn of the century.

One of the most obvious ways of attempting to deal with the failure of the Langevin equation (8) when faced with accurate data from the far infrared was to add a term on the left-hand side to mimick the effect of an extra torque generated by the immediate surroundings of a diffusing molecule. These surroundings are, of course, other diffusing molecules, which form a cage which itself diffuses with time. To put these ideas in simple mathematical form several assumptions were made which can only be justified by working out their consequences mathematically and comparing with experimental data in the complete range of available frequencies, not just in the dielectric range where every model gives closely similar results, difficult to distinguish from the bell-shaped curve, giving an illusion of explanation. The complete range extends from static (zero frequency) to the THz, as much as 14 frequency decades.

P. The Harmonic Approximation

The extra torque on the left-hand side of the Langevin equation is assumed to take the form

$$\frac{\partial V}{\partial \theta} = V_0 \sin \theta \quad (31)$$

If the angle θ is below about five degrees, then the sine can be replaced by the angle itself, so that the rotational Langevin equation becomes

$$I\ddot{\theta} + \beta_R\dot{\theta} + V_0\theta = \lambda \quad (32)$$

The extra torque comes from assuming that the potential energy generated by torsional oscillation of a diffusing molecule in a cage of neighbors is a simple cosine. Differentiation of the cosinal potential energy with respect to angular displacement gives the torque. For small angles the sine is approximated by its argument, so that torsional oscillation occurs at the bottom of a potential "well". Implicit in the whole exercise are at least two further hidden assumptions, that the rotational diffusion of the molecule is statistically uncorrelated to its own translation, and that the torsional oscillation takes place in a plane, so that the nonlinearities of the Euler equations do not complicate the mathematics. Given all these assump-

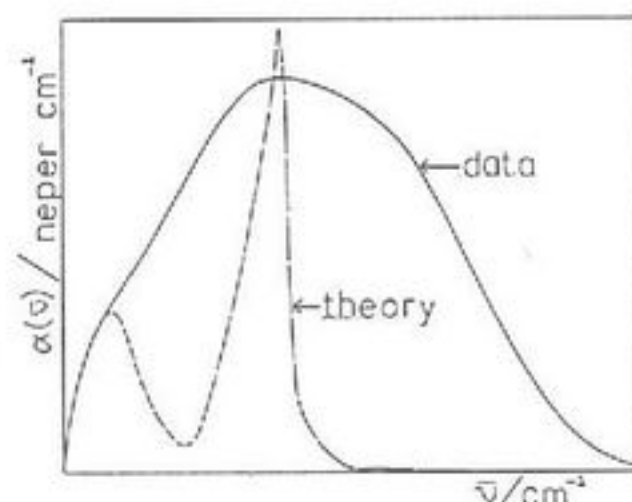


Figure 6. An attempt at reproducing the far infrared power absorption of a dipolar liquid with a harmonic approximation or with the planar itinerant oscillator of Calderwood and Coffey (schematic).

tions, the Langevin equation (32) may be solved by Laplace transformation for the far infrared power absorption coefficient and the dielectric complex permittivity. The mathematical expressions for these optical coefficients as a function of frequency (the spectra) are very complicated^{1,4} functions of the friction coefficient β_R and the barrier height or well depth V_0 . These two parameters cannot, however, be expressed in terms of the fundamental physical constants and are therefore empirical.

We arrive at the conclusion that the theory of rotational diffusion must be supplemented by an extra torque in order to provide even a qualitative theoretical explanation for experimental data in the electromagnetic frequency range from static to far infrared. This is necessarily an empirical procedure, because there are two parameters which must be varied for best fit of experiment and theory. A typical result of such an approach is illustrated in Fig. 6. The low-frequency part of the data range is matched satisfactorily, as is the case for many models of this type, but in the far infrared the harmonic approximation typically gives much too sharp a result. It provides limited progress from the Debye plateau, and approximations of the Sack continued fraction, the various "inertial corrections" of Debye's theory.

Q. The Itinerant Oscillator

This was developed initially by Hill³⁰ and Wyllie.³¹ In the early 1970s, versions of the theory were first tested against far infrared data.^{12,32} A later and simpler planar version was developed³³ which provided a clear explanation of its fundamental principles. All of the various models rely heavily on the theory of rotational diffusion, and decorrelate molecular rotation from molecular translation. The planar version³³ was developed to avoid the mathematical complexities of three-dimensional rotational diffusion.

The itinerant oscillator considers diffusion to be superimposed on oscil-

lation. For rotational motion the latter is torsional oscillation ("libration") in a cage of nearest neighbouring molecules which is assumed to diffuse throughout the medium as a rigid entity. A molecule simultaneously diffuses and librates within the cage. It is assumed that a Langevin equation can be used to describe the diffusion of the outer cage. The theory³³ of Calderwood and Coffey also assumes that the rotational diffusion of both cage and molecule can be approximately planar, and that there is no friction between the cage and inner molecule.

With these assumptions, the Langevin equation of the cage is

$$I_1 \ddot{\psi} + I_1 \beta \dot{\psi} - I_2 \omega_0^2 (\theta - \psi) = I_1 \dot{W} \quad (33)$$

linked to the oscillatory diffusion of the inner molecule

$$I_2 \ddot{\theta} + I_2 \omega_0^2 (\theta - \psi) = 0 \quad (34)$$

Here I_1 is the effective moment of the cage (the "annulus" in two dimensions); I_2 is the moment of inertia of the inner molecule (the "disk" in two dimensions); θ and ψ are angular variables of the motion defined as follows. θ is the time-dependent angular displacement between the inner molecule's dipole moment and the applied electric field which measures the polarization in the technique of dielectric spectroscopy. ψ is the displacement between a point on the rim of the annulus and this electric field direction. The torque on the outer annulus due to Langevin friction is $I_1 \beta \dot{\psi}$ and the random force on the annulus is $I_1 \dot{W}$. Note that the equations of this, the simple planar itinerant oscillator, can be written as

$$I_1 \ddot{\psi} + I_1 \beta \dot{\psi} + I_2 \ddot{\theta} = I_1 \dot{W} \quad (35)$$

which is a simple Langevin equation with an added inertial term $I_2 \ddot{\theta}$ on the left-hand side.

The mathematical solution of Eq. (35) is elaborate and incomplete, despite its physical simplicity. Full descriptions are given in the specialist literature.^{1-4,33} Solutions are available, however, for the acf of the angular velocity, $\dot{\theta}$, of the encaged molecule; for the orientational acf, essentially the Fourier transform of the dielectric loss; and for the rotational velocity acf from the model, the Fourier transform of the far infrared spectrum. Using these results, the combined dielectric and far infrared spectra can be modelled with two parameters: β , the friction coefficient on the cage, and the harmonic torsional oscillation frequency, ω_0 , of the itinerant oscillator, the encaged molecule.

R. Experimental Testing of the Itinerant Oscillator

The model has been tested thoroughly with far infrared and dielectric data (see Sections 2–4). These were the first tests carried out on a theory of rotational diffusion qualitatively able to account for new spectral features in the far infrared. The theory contains β and ω_0^2 as parameters, and also the ratio I_1/I_2 , which are empirical. This reflects the somewhat superficial nature of the original Debye approach of 1913, the ad hoc mixture of concepts of the traditional approach to molecular dynamics. The problem of comparing the theory with far infrared data was tackled^{34–40} in several ways, using the necessary broad sweep of data over the microwave and far infrared regions in sample liquids such as dichloromethane, of C_{2v} point-group symmetry. In one method the three parameters were optimized freely with least-mean-squares simultaneous minimization. This force fit to the complete frequency sweep of available data exposed a fundamental flaw in the Calderwood Coffey variation of Debye's original theory, in that the moment of inertia of the annulus had to be about eight times *smaller* than that of the disk for most samples of molecular liquid. This ratio is the wrong way around, because the cage is more massive than the encaged molecule. For reasonable values of the parameters β and ω_0^2 the physically expected ratio $I_1/I_2 \approx 10$ always produced a very sharp theoretical peak in the far infrared reminiscent of the simple harmonic librator, Eq. (32). This was much sharper than the experimentally observed absorption. This problem defines the severe limitations of the original theory.³³ Other methods of comparison provided the same result, for example the friction coefficient, β , was estimated numerically by making sure that the theory produced peaks at the right far infrared and microwave frequencies. This method again produced the unphysical ratio of moments of inertia.

This defect was remedied^{41–43} in 1987 by removing the assumption that the interaction between molecule and cage is harmonic and frictionless. Unfortunately, the remedy introduces a new parameter, the friction coefficient between the cage and the encaged molecule. However, the use of four parameters finally manages to provide a fit to observed data over the complete frequency range with physically acceptable moment of inertia ratios. The new Langevin equations are

$$I_1 \ddot{\psi} + I_1 \beta_1 \dot{\psi} - \mu F \sin(\theta - \psi) = \lambda_1 \quad (36)$$

$$I_2 \ddot{\theta} + I_2 \beta_2 \dot{\theta} + \mu F \sin(\theta - \psi) = \lambda_2 \quad (37)$$

where β_2 is the new friction coefficient. These are simple linked Langevin equations, still closely based on rotational diffusion theory, carrying with them all its original flaws.

1. There are too many empirical parameters for the data available from the microwave and far infrared. It would require the simultaneous use of four independent data sources to define the four parameters, and this exercise has never been attempted.
2. There is a loss of physical realism in an effort to retain mathematical tractability, that is, the equations are written down so that they can be solved.
3. The fundamental dynamics neglect the Euler cross terms, because these are mathematically intractable.
4. These equations retain the drastic assumptions made at the turn of the century that rotation and translation are decorrelated. Contemporary computer simulation has exposed this as an erroneous assumption which produces an illusory understanding of diffusion.
5. Even with these assumptions, Eqs. (36) and (37) can be solved only in restricted special cases, and then only by recourse to the equivalent equations of probability diffusion, the Klein/Kramers equations.^{41–43} Solutions are available for equal friction coefficients only.
6. With the free use of four parameters, even if a solution could be found for unequal friction coefficients, the equations fail if exposed to a sufficiently broad range of viscosity. In supercooled molecular liquids, for example, they cannot produce the observed split in the dielectric loss known^{1–4} as the α and β processes, whose far infrared adjunct is the γ process. These three processes cover a very broad frequency range and exhibit a complexity of behaviour which no simple diffusion theory could describe.
7. The itinerant oscillator cannot follow phase changes, and neither can any theory based on Debye rotational diffusion.
8. The equations of the itinerant oscillator bear no direct or reasonable relation to the fundamental equations of classical mechanics, or statistical mechanics (the Liouville equation). This is so in any theory of rotational diffusion which does not use the memory function approach developed by Mori in 1965 and described in the specialist literature.^{1–4}

The itinerant oscillator theory is an empirical description of N body dynamics which can "force-fit" data over a restricted range of viscosity. It is not tenable as a fundamental theory, and for this we need computer simulation.

S. Relationship of the Itinerant Oscillator with the Liouville Equation

We consider the Mori equation (6), a form of the Liouville equation. This describes the conditional probability density function for all positions and momenta of the molecules in the ensemble under consideration. It can be written specifically for molecules in a molecular environment, rather than for Brownian motion. In principle, the Langevin equation is less useful to molecular dynamics than the rigorous Liouville equation. However, the latter is more suitable for use in the Mori form than in the form originally devised by Liouville in 1838.

Mori used projection operators to develop equation (6), which is formally the same as the Liouville equation. To illustrate the connection between the Mori equation and the itinerant oscillator of Eq. (35) consider the molecular angular velocity constrained to planar rotational dynamics as implemented by Debye. Assume that the Mori column vector \mathbf{A} can be replaced by the single scalar entry $\dot{\theta}$, the time derivative of the two-dimensional angular displacement. This implies that the Mori resonance operator vanishes, which means physically that the relation between single molecule diffusion and cooperative effects generated by this diffusion is lost. With these assumptions the Mori equation reduces to

$$\ddot{\theta}(t) = -\int_0^t \phi(t-\tau)\dot{\theta}(\tau) d\tau + F_{\dot{\theta}}(t) \quad (38)$$

where ϕ is the memory function for two-dimensional Debye-type rotational diffusion. Inspection of this equation reveals that it reduces to the inertia-corrected Debye equation (27) when the memory function is a delta function in time

$$\phi(t-\tau) = \delta(t-\tau) \quad (39)$$

More generally, however, Mori showed that the integro-differential equation (38) is the fit in a chain of similar equations, whose first members are

$$\dot{\phi}(t) = -\int_0^t \phi_1(t-\tau)\phi(\tau) d\tau + F_1(t) \quad (40a)$$

$$\dot{\phi}_1(t) = -\int_0^t \phi_2(t-\tau)\phi_1(\tau) d\tau + F_2(t) \quad (40b)$$

The memory function is itself governed by a like equation, and so on for

more indices. The Laplace transformation (L_A) of the chain of equations (40) produces the well known Mori continued fraction expansion of the angular velocity acf

$$L_A\left(\frac{\langle\dot{\theta}(t)\dot{\theta}(0)\rangle}{\langle\dot{\theta}^2\rangle}\right) = C(p) = \frac{1}{p + \frac{K_0}{p + \frac{K_1}{p + K_2 \dots}}} \quad (41)$$

where K_0 , K_1 , and K_2 , are constants.

There is a relation between this second approximant of this continued fraction and the Calderwood-Coffey itinerant oscillator, which was first derived in 1976.⁴⁴ The second approximant of the continued fraction (41) and the equivalent expression from the itinerant oscillator equations³³ for the same acf are formally identical. The itinerant oscillator equations (35) are therefore approximations at an early stage to the Mori equation (38), truncating the continued fraction after only two approximants. In the same way, the 1987 version of the itinerant oscillator is equivalent to a truncation procedure at the same approximant of a matrix continued fraction.

T. The Grigolini Continued Fraction

We have seen that the Debye theory of rotational diffusion, and its close relative, the itinerant oscillator, are special cases of the Liouville equation written in terms of a continued fraction. Grigolini¹⁻⁴ has shown that the continued fraction has a deeper significance in classical and wave mechanics.

Grigolini developed the continued fraction from the "Heisenberg equation"

$$\frac{\partial A}{\partial t} = L \times A \quad (42a)$$

which is equivalent to the Mori equation in statistical mechanics. Equation (42a) is also a Liouville equation for the general dynamical variable A , a stochastic or random variable, not purely deterministic. The equivalent "Schrödinger equation" in this analogy is the Liouville equation applied directly to the probability density $\rho(\mathbf{a}, \mathbf{b}, t)$

$$\frac{\partial \rho(\mathbf{a}, \mathbf{b}, t)}{\partial t} = L\rho(\mathbf{a}, \mathbf{b}, t) \quad (42b)$$

The operator L is the effective Liouvillian

$$L = L_a + L_b + L_1 \quad (43)$$

made up of three parts, operating on the stochastic variables \mathbf{a} and \mathbf{b} of the equation (42b). The third part, L_1 , represents the statistical interaction between the two sets of variables denoted by \mathbf{a} and \mathbf{b} .

The starting point for the Grigolini continued fraction is Eq. (42b), which is obtained by working directly with a variable A of the set \mathbf{a} , and then building its time correlation function

$$\Phi(t) = \frac{\langle A(0)A(t) \rangle}{\langle A^2 \rangle_{eq}} \quad (44)$$

where

$$A(t) = e^{\Gamma t} A(0); \quad \Gamma = L^\times$$

$$\langle \quad \rangle_{eq} = \int dA d\mathbf{b}(\dots) \rho_{eq}(A, \mathbf{b})$$

Here ρ_{pq} is the equilibrium probability distribution. Analogously with Heisenberg quantum mechanics, the time-correlation function is the scalar product, a running time, or ensemble, average

$$\Phi(t) = \frac{\langle A | A(t) \rangle}{\langle A | A \rangle} \quad (45)$$

In analogy with quantum mechanics the Mori continued fraction is obtained by choosing the basis set for the expansion of the operator L^\times of Eq. (42a). The basis set is built up of repeated projections on to subspaces of the complete Hilbert space. Grigolini generalises Mori's treatment of the same problem with a biorthogonal basis set. This leads to the integrodifferential equation

$$\frac{d}{dt} \Phi(t) = \lambda_0 - \Delta_1^2 \int_0^t \Phi(\tau) \Phi_1(t - \tau) d\tau \quad (46)$$

for $\Phi(t)$. Here

$$\frac{d}{dt} \Phi_k(t) = \lambda_k \Phi_k(t) - \Delta_k^2 \int_0^t \Phi_k(\tau) \Phi_{k+1}(t - \tau) d\tau \quad (47)$$

and to the continued fraction in Laplace space

$$\Phi(p) = \frac{1}{p - \lambda_0 + \frac{\Delta_1^2}{p - \lambda_1 + \frac{\Delta_2^2}{\dots \frac{\Delta_{n-1}^2}{p - \lambda_{n-1} + \Delta_n^2 \Phi_n(p)}}}} \quad (48)$$

This has the same form as the Mori and Sack continued fractions, but is more general in applicability.³ In Eqs. (46)–(48) λ is the equivalent of the Mori resonance operator, Φ_n the Grigolini memory function, and Δ_n^2 can be related to spectral moments and determined unequivocally in some cases. There is therefore a well-understood relation between the fundamental equation of motion and the less general diffusion equations, which they approximate. The itinerant oscillator is an approximant of the Grigolini continued fraction.

U. The Statistical Correlation between Rotation and Translation

The development so far has been restricted to separate consideration of translational and rotational diffusion. From first principles it is clear, however, that one form of motion occurs simultaneously with the other in molecular dynamics. Computer simulations of the last 10 years have shown conclusively that there is statistical correlation of many forms between one type of motion and the other in molecular ensembles. There are important hydrodynamic effects caused by the interaction between rotation and translation in fluid materials. On the molecular level none of these effects had been considered in the traditional approach prior to the use of computer simulation. The precise statistical interrelation between the linear and angular velocity of an asymmetric top molecule diffusing in three dimensions is a major unsolved problem of diffusion theory.

There have been several attempts at extending the theory of diffusion

to describe the "roto-translation" of molecules rather than separated rotational and translational diffusion of pollen particles. These have to deal with elementary considerations such as the following. Let \mathbf{u} be a unit vector joining the center of mass of a molecule to one of its atoms. Let the centre of mass velocity of the diffusing particle be \mathbf{v} and the linear velocity of the atom \mathbf{v}_a . If $\boldsymbol{\omega}$ is the angular velocity of the complete molecule, assumed rigid, then

$$\mathbf{v}_a = \mathbf{v} + \frac{1}{2}\boldsymbol{\omega} \times \mathbf{u} \quad (49)$$

The acf of \mathbf{v}_a therefore contains information on both linear and angular velocities simultaneously, and the acf can be extended as follows

$$\langle \mathbf{v}_a(t) \cdot \mathbf{v}_a(0) \rangle = \langle (\mathbf{v}(t) + \frac{1}{2}\boldsymbol{\omega}(t) \times \mathbf{u}(t)) \cdot (\mathbf{v}(0) + \frac{1}{2}\boldsymbol{\omega}(0) \times \mathbf{u}(0)) \rangle \quad (50)$$

Using the fundamental kinematic relation²⁶ between the rotational velocity $\dot{\mathbf{u}}$ and the orientational unit vector \mathbf{u}

$$\dot{\mathbf{u}} = \boldsymbol{\omega} \times \mathbf{u} \quad (51)$$

The expansion of the acf in Eq. (50) contains the *cross-correlation function* (ccf)

$$C_{\dot{\mathbf{u}}\mathbf{v}} = \langle \dot{\mathbf{u}}(t) \cdot \mathbf{v}(0) \rangle \quad (52)$$

between the rotational and linear velocities of the diffusing molecule. This ccf exists directly in the laboratory frame (X, Y, Z). An example, from a recent computer simulation of liquid water, is shown in Fig. 7.

Computer simulations have shown⁴⁵ that there are many ccf's such as this, involving rotational and translational dynamics simultaneously at the molecular level. These are governed by powerful symmetry laws^{1,46,47} of time reversal, parity reversal, and point group theory in frames (X, Y, Z) and (x, y, z). These laws will be developed later in this chapter into group theoretical statistical mechanics (gtsm). They allow the existence of some ccf's but forbid that of others in both frames of reference. One of the ccf's disallowed by parity reversal symmetry in frame (X, Y, Z) is

$$C_{\boldsymbol{\omega}\mathbf{v}} = \langle \boldsymbol{\omega}(t) \cdot \mathbf{v}(0) \rangle = 0 \quad (53)$$

However, if we switch in to the frame (x, y, z) which is fixed in the molecule, and moves with it, this type of ccf becomes visible, and other types of ccf appear⁴⁷⁻⁵² which we cannot see in frame (X, Y, Z). These

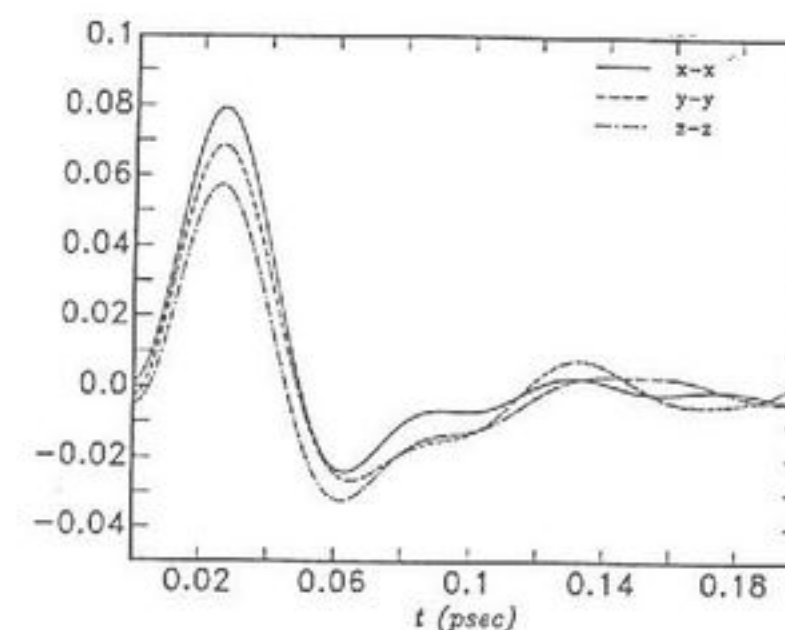


Figure 7. Illustration of the laboratory frame cross-correlation function (ccf) $C_{\dot{\mathbf{u}}\mathbf{v}}$ obtained from a recent super-computer simulation of liquid water by Evans, Lie and Clementi, IBM, Kingston.

have all been traced in the last few years with the help of computer simulation.^{45,47-53} If the frame (x, y, z) is defined as that of the principal molecular moments of inertia, it is simultaneously rotating and translating with respect to frame (X, Y, Z), (Fig. 8). Every molecule has its frame (x, y, z). For each molecule, one frame can be matched with the other by a series of rotations, which define the Euler angles, for example. Any scalar, vector, or tensor quantity can be defined with respect to either frame.

The linear velocity, \mathbf{v} , for example, has the components $v_X, v_Y,$ and v_Z in frame (X, Y, Z) which can be rotated into frame (x, y, z) with the use of the three unit vectors $u_x, u_y,$ and u_z defined in the axes $x, y,$ and z of the frame (x, y, z) through the rotation equations

$$v_x = v_X u_{xX} + v_Y u_{xY} + v_Z u_{xZ} \quad (54)$$

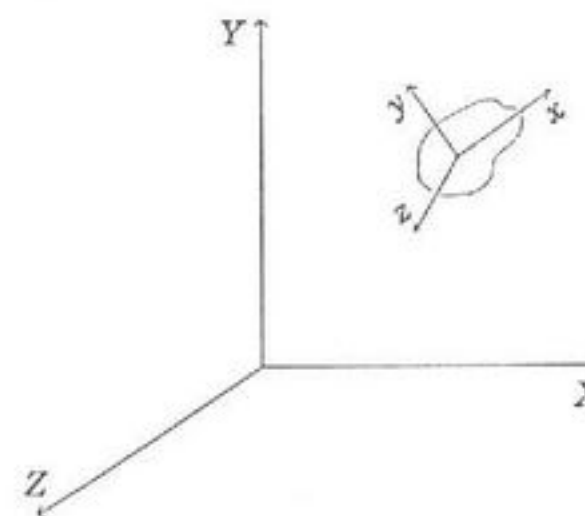


Figure 8. Illustration of frames (X, Y, Z) and (x, y, z) for a molecule diffusing in three dimensions.

$$v_y = v_X u_{yX} + v_Y u_{yY} + v_Z u_{yZ} \quad (55)$$

$$v_z = v_X u_{zX} + v_Y u_{zY} + v_Z u_{zZ} \quad (56)$$

In matrix notation these equations are

$$\begin{bmatrix} v_x \\ v_y \\ v_z \end{bmatrix} = \begin{bmatrix} u_{xX} & u_{xY} & u_{xZ} \\ u_{yX} & u_{yY} & u_{yZ} \\ u_{zX} & u_{zY} & u_{zZ} \end{bmatrix} \begin{bmatrix} v_X \\ v_Y \\ v_Z \end{bmatrix} \quad (57)$$

so that \mathbf{v} in one frame is related to \mathbf{v} in the other by a transformation matrix. Any vector can be transformed from one frame into the other in a similar way. There are major advantages of considering both frames. For example,

1. Group theory can be applied in both frames, revealing a great deal in frame (x, y, z) that is hidden in frame (X, Y, Z) . Point-group theory has been highly developed in other branches of chemistry and spectroscopy, and the complete range of results can be used directly to study molecular diffusion, culminating in the three principles of gsm (Sections VII and VIII).

2. The ccf's allowed by symmetry in either frame can be investigated for their time dependence by computer simulation, and increasingly, by experimental methods. These produce the details of the time dependence of each ccf for any molecular symmetry. The simulation can also be extended to vibrating and flexible molecules. It is generally applicable in all molecular point-group symmetries.

Steps 1 and 2, taken in the past 5 years or so, lead to advances in our understanding of molecular diffusion processes.

V. The Challenge to Traditional Diffusion Theory

The traditional approach has been overtaken by computer simulation and group theory. There has been a sudden increase in understanding based on group theoretical statistical mechanics. The traditional approach is challenged with describing the data now available from computer simulation, and also obtainable experimentally, through processes described in Sections VII and VIII. These are challenges posed by the much older classical equations of motion devised by Newton and Euler:

1. There are many different types of cross correlation that can be used to describe the diffusion of molecules in a molecular environment. These

exist in frames (X, Y, Z) and (x, y, z) and in the latter are governed by the molecular point-group symmetry. They always accompany a range of acf's in both frames which the theory must describe consistently. Some of the acf's and ccf's are experimentally observable. The theory of diffusion must be capable of describing the complete set of correlation functions from simple starting assumptions.

2. The Langevin equation is incapable of more than a general qualitative description, and must be modified to deal with new data from spectra and computer simulation.

3. The traditional rotational and translational diffusion theories are mutually exclusive. The original treatment of Debye left out the inertial term, causing a drastic failure in the far infrared. Reinstating this does not produce the observed far infrared spectrum. There is no rigorous justification for the use of simple rotational diffusion theory in the description of molecular diffusion processes.

4. The various itinerant oscillator theories attempt to extend the validity of rotational diffusion by ad hoc addition of torque terms to the rotational Langevin equation. This is essentially an empirical procedure which runs into difficulties caused by unknown parameters and great mathematical complexity. Some versions are further restricted by deliberate neglect of the nonlinear components of the Euler equations of motion.

5. The Langevin equation, and the diffusion equations in general, are not fundamental equations of motion such as the Liouville equation, and cannot be obtained from the latter without crude approximation.

6. Doob²⁰ showed as early as 1942 that there are inherent inconsistencies in the simple Langevin equation. The velocity may have no proper time derivatives. The velocity acf from the Langevin equation is an exponential decay, which is not differentiable at $t=0$. The time expansion of these acf's violates the rules of classical statistical mechanics,¹ which imply that a classical acf must be time-even. Significantly, Doob showed that the Langevin equation is self-consistent only if expressed in the integral form

$$v(b) - v(a) = -\beta_v \int_a^b v(t) dt + B(b) \quad (58)$$

where

$$B(b) - B(a) = \sum_{k=1}^n (B(t_k) - B(t_{k-1}))$$

This is reminiscent of the Mori equation (6). Doob anticipated this equation with its memory function replaced by a constant friction coefficient. The random force B in Eq. (58) must be a Wiener process.¹ The ramifications of this are described in the specialist literature,¹⁴ but the mathematical niceties do not affect the drastic failure of the equation in the far infrared.

7. Most challenging is the failure of contemporary diffusion theory to describe the simultaneous translational and rotational dynamics of a molecule diffusing in three dimensions. This limitation is built in at the most fundamental stage of the theory, and has been exposed to view by computer simulation. Molecular rotation and translation are always correlated, even in spherical tops,^{56,57} and the cross-correlation is governed in general by point-group theory,⁵⁸ and fundamental symmetry laws of physics. All known generalizations of the Langevin equation run into considerable difficulty when attempts are made to account consistently for the sets of nonvanishing ccf's and acf's generated by the simple fact that a molecule simultaneously rotates and translates. One can question the usefulness of the concept of diffusion at the most basic level. There is no known solution from diffusion theory at the time of writing which is able to describe the data from spectra and computer simulation without approximation, complexity, and overparameterization caused by empiricism. Computer simulation has advanced well beyond the tight boundaries of these theories. Computer simulation is a simpler and more consistent approach, because it relies on fundamental equations of motion. It has advanced to the stage where description of spectra is possible using these equations. Some of these spectra are described in the next section.

II. KEY EXPERIMENTS

A century ago, the Michelson–Morley experiment proved the fallacy of the luminiferous ether (lichtäther), leading to the great advances in the theory of relativity made by Lorentz, Fitzgerald, and Einstein. Einstein's scientific contemporaries based their theories of diffusion on his work of 1905, reviewed in Chapter 1, explaining Brownian motion in molecular terms. The probability diffusion equations from their work foreshadowed the emergence of wave and quantum mechanics in the 1920s.

The opening up of the far infrared by Michelson interferometry had a similar effect on the theory of diffusion. The Michelson interferometer, and the precision it brings to the measurement of the speed of light, destroyed the theory of the luminiferous ether, forcing the great advances in relativity theory. In the late 1960s the same interferometric technique

was used to show up severe shortcomings in the received wisdom pertaining to molecular diffusion. In this chapter, the key late twentieth century observations and techniques are described which led to this turning point. Signs of the old theory's limitations showed up rapidly and almost contemporaneously in several different spectroscopic observations. Each of these is described with a view to explaining the need for computer simulation as a guide to further progress in this field.

A. Interferometric Spectroscopy of Molecular Liquids

From its inception in 1913 to the mid-1950s, the data available to test the theory of rotational diffusion were confined to spot frequencies in the range from static to the microwave (GHz). The experimental techniques for obtaining the dielectric loss of a molecular liquid as a function of frequency varied according to the frequency range of interest. A laboratory would be equipped for a total frequency sweep of several decades on the logarithmic scale. This would be accomplished with radio frequency bridges for the Hz to kHz range, Wayne Kerr bridges and so on to the MHz range, microwave apparatus in the GHz range. Microwave measurements were laborious and costly, needing waveguides, klystrons, generators, and other specialized apparatus. Measurements were typically possible at 2, 4, and 8 mm, using frequency doubling. Sweep-frequency apparatus⁵⁹ is a recent innovation which allows a spectrum to be measured in the MHz range of frequencies. Before that, spot frequencies only were available. A plot of dielectric loss or permittivity against the logarithm of frequency consisted of isolated points, widely separated on the frequency scale by regions about which nothing was known. Spectra were taken at very low resolution, in other words, in the hope of finding enough information to test a theory of diffusion. The overall objective was the study of molecular dynamics at low frequencies.

These data could not distinguish between different theories of diffusion without information at high frequency and better spectral resolution, obtainable in the GHz to THz (far infrared) frequency range. Spot frequencies in the kHz to MHz range, however accurate, cannot tell the difference between a flawed theory such as rotational diffusion (Section I) and more rigorous descriptions based on the fundamental equations of motion, for example Mori and Grigolini continued fractions and computer simulation. The reasons for this were discussed in Section I and can be traced to the tendency of the orientational acf to become exponential as $t \rightarrow \infty$ or at low frequencies. A complete description of the molecular diffusion process in liquids needs the far infrared frequency region as a guideline.

Some of the first indications of the way that molecular liquids absorb in the far infrared (about $2\text{--}250\text{ cm}^{-1}$, where it overlaps with the infrared),

were obtained by Poley in 1955.⁶⁰ Using spot frequency measurements he found that the effective dielectric loss of dipolar liquids in the very high-frequency end of the GHz range was consistently above the value expected from the Debye rotational diffusion theory, despite the fact that the latter seemed to produce good agreement with dielectric loss and permittivity data at lower frequencies. Poley's measurements were however laborious to repeat in other laboratories and were viewed with uncertainty. The true significance of his data was realized fully after the passage of a decade,¹² which saw the rapid development^{1,28,29} of far infrared Michelson interferometry. Computers were harnessed to arrive numerically at the far infrared power absorption spectrum from the interferogram produced by moving a mirror in one arm of the Michelson interferometer. The process of obtaining the spectrum from the interferogram is Fourier transformation (Section I), and for this reason the technique is often known as Fourier transform spectroscopy.

B. The Basic Principles of Fourier Transform Spectroscopy⁶¹ in the Far Infrared

The Michelson interferometer is a simple optical device driven essentially by a light source which produces broad band radiation according to Planck's Law. This is black-body radiation,²⁹ the intensity of which decreases rapidly with increasing wavelength. The relation between wavelength (λ) and wavenumber ($\bar{\nu}$) is a simple inverse

$$\bar{\nu}\lambda = 1 \quad (59)$$

so that in the far infrared, the intensity of black-body radiation is minute in comparison with, for example, the visible. This simple consequence of Planck's Law means that conventional prism or grating-based spectrometers, of utility in the conventional infrared range just below the visible, become difficult to use with accuracy as the far infrared range is approached. The two important frequency decades from 1 to 10 cm^{-1} and from 10 to 100 cm^{-1} are particularly difficult for grating spectrometers. The great advantage of the Michelson interferometer in the far infrared is that it utilizes the whole of the available radiation from the light source. This radiation is guided after collimation on to a beam splitter which produces two beams at right angles, one by refraction through the beam splitter, and the other by reflection. By positioning the beam splitter at 45° to the incoming radiation from the light source, the refracted and reflected beams travel at right angles to the two mirrors of the Michelson interferometer.^{1,28,29} The two beams are reflected back along their paths, which recombine at the beam divider and optically interfere constructively

or destructively according to phase difference. The resultant electromagnetic radiation is either refracted through the beam splitter into an optical detector or reflected back into the source.

C. The Interferogram

The interferogram is the intensity of electromagnetic radiation reaching the detector as the function of the distance of one mirror from that point at which both are equidistant from the beam divider. To build up an interferogram, one mirror is therefore displaced in the interferometer, either by stepping it mechanically or electrically, or moving it continuously. If the two mirrors are equidistant from the beam splitter, the two beams from each arm of the interferometer are exactly in phase and interfere constructively. If the mirror to beam divider distance in one arm is displaced by only half a wavelength then destructive interference occurs. With monochromatic radiation entering the interferometer the interferogram is a simple cosine. With polychromatic radiation it is a complicated pattern of maxima and minima, whose Fourier transform gives the spectrum. The power absorption coefficient of the molecular liquid under study is obtained by placing a carefully measured thickness of the liquid just before the detector, measuring its interferogram, and repeating the process with a slightly thicker specimen of liquid. The instrument function of the interferometer is compensated for by taking a ratio of the Fourier transform of the thick to the thinner liquid samples. The far infrared power absorption coefficient is then defined as

$$\alpha(\bar{\nu}) = \frac{1}{d} \log_e \frac{I_0}{I} \quad (60)$$

where d is the increment in liquid thickness, and I_0/I the ratio of radiation intensity at the detector for each frequency.

The technique is now well documented^{1,28,29,61} and Fourier transform spectrometers dominate the market.⁶² The interested reader is referred to this literature for further details. Some technical steps are necessary to go from the prototype optical set-up to a powerful instrument such as the Bruker IFS 113v⁶² or those marketed by Nicolet or Grubb Parsons and several other companies. These steps include the following:

1. The inbuilt computers and software of the contemporary Fourier transform spectrometer are designed to include numerical compensation for discrete sampling of the interferogram, and finite distance travelled by the mirror. These artifacts are treated respectively with the apodisation (sampling) function and the window function. The former is a series of

delta functions and the latter a specially designed mathematical function which compensates for spurious oscillations caused by the unavoidable truncation of the interferogram.

2. The resolution of the spectrometer is determined by the maximum amount (Δd) by which the mirror can be displaced, and is given by

$$\Delta \bar{\nu} = \frac{1}{2\Delta d}$$

Fourier transform spectrometers provide very high resolution across a wide frequency range of four decades.

3. The spectral range of the Fourier transform spectrometer is determined essentially by the stepping distance, and to maximize the range and minimize the problem known as "folding" the mirror stepping distance is minimized. Different spectral ranges require different sources, optical materials, and beam splitters, and spectrometers are automated for different ranges. Most instruments cover the very far infrared to the visible, including the whole of the infrared range.

4. Another major advantage is that the whole range is covered at constant, high-resolution, unlike grating spectrometers.

5. With the use of sensitive liquid helium cooled detectors the upper end of the microwave range can be reached (about 2 cm^{-1}). This is 5 mm in terms of wavelength, or 60 GHz in frequency. Conventional waveguides reach 8 mm typically. The present author has obtained comfortable overlap⁶³⁻⁶⁸ in several different systems using the accurate designs pioneered at the National Physical Laboratory in the U.K. and marketed by Grubb-Parsons and Specac. The overlap was accurate both in terms of frequency and power absorption coefficient (the spectral ordinate in neper cm^{-1}).

D. Key Spectral Data: The Challenge to Diffusion Theory

The challenge is exemplified by the data available for the simple asymmetric top, dichloromethane.^{1,3,4} The complete electromagnetic spectrum¹⁻⁴ of this asymmetric top can stretch over many frequency decades, the more the greater the viscosity. This signals diffusion processes that evolve over an immense span of time, from picoseconds to years. In the dilute gaseous condition the far infrared spectrum of dichloromethane is a series of rotational lines⁶⁹⁻⁷¹ generated by the Schrödinger equation for a freely rotating molecule in an ensemble. The intensity distribution of these lines is governed by the laws of statistical mechanics. The full extent of the challenge to molecular diffusion theory can be gauged when we consider carefully what happens as the gas is condensed into a liquid, and this is

cooled and then supercooled below its normal freezing point at a given pressure.

E. Condensation of Gas to Liquid

As a dilute gas of dichloromethane is compressed, the rotational lines broaden and merge.⁷²⁻⁷⁵ The wave functions of the free molecular rotators are affected by the fields of force of other molecules. The energy associated with a particular quantum state of the free rotator is no longer defined sharply at one frequency (energy value) only. The disturbance produced by the fields of neighbouring molecules produces a spread of frequencies around each quantum line of the free rotor. The spectrum begins to merge into a broad band, and there is a transition from quantum mechanical descriptions to those based on statistical mechanics.

One of the problems with the theory of diffusion becomes apparent when the spectrum has merged into a broad band in the far infrared. The original quantum structure has disappeared. The statistical description of the broad band rests on building up an acf (Chapter 1) from the kinematic equation¹

$$\dot{\mathbf{u}}^{(i)} = \boldsymbol{\omega}^{(i)} \times \mathbf{u}^{(i)} = \mathbf{A}^{(i)} \mathbf{u}^{(i)} \quad (61)$$

written separately for each particle $i = 1, \dots, N$, where N is the total number of molecules in the liquid. The orientational acf is the running time average

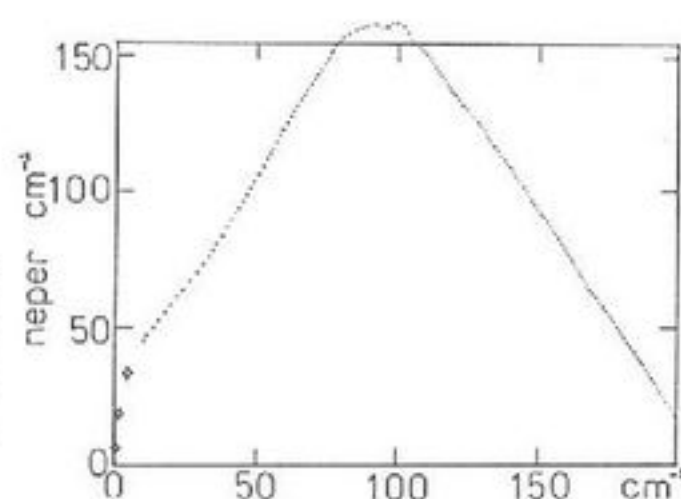
$$\langle \mathbf{u}(t) \cdot \mathbf{u}(0) \rangle = \frac{1}{N} \sum_{i=1}^N (\mathbf{u}^{(i)}(0)^T \exp(\mathbf{A}^{(i)} t)) \mathbf{u}^{(i)}(0) \quad (62)$$

When N is of the order of Avogadro's Number (6.023×10^{23}) we can replace the sum by an integral involving two types of averaging, over the initial orientations of the dipoles and the second over the angular velocity probability distribution, which by classical statistical mechanics⁷⁶⁻⁷⁸ is a Maxwell-Boltzmann distribution

$$P(\boldsymbol{\omega}) = Z \exp \left\{ -\frac{1}{2kT} (I_x \omega_x^2 + I_y \omega_y^2 + I_z \omega_z^2) \right\} \quad (63)$$

Here the I 's are the three principal moments of inertia and the ω 's are the three components of the molecular angular velocity in the principal moment of inertia frame (x, y, z) fixed in the molecule (Chapter 1). Z is

Figure 9. The low frequency absorption of liquid dichloromethane in the frequency range from static to about three hundred wavenumbers (the high frequency limit is the far infra-red) (schematic).



a constant. For the asymmetric top the orientational acf of the classical free rotor follows as¹

$$\langle \mathbf{u}(t) \cdot \mathbf{u}(0) \rangle = \frac{1}{3} \int d^3\omega P(\omega)(1 + e^{i\omega t} + e^{-i\omega t}) \quad (64)$$

If the three moments of inertia of the molecule are equal (the spherical top), this expression reduces to

$$\langle \mathbf{u}(t) \cdot \mathbf{u}(0) \rangle = \frac{1}{3} + \frac{2}{3} \left(1 - \frac{kTt^2}{I}\right) \exp\left(-\frac{kTt^2}{2I}\right) \quad (65)$$

Now this expression, derived from the purely kinematic equation (61), is completely unlike the one derived from the three dimensional diffusion of the spherical top from the rotational Langevin equation (8) after the Debye theory⁵ has been corrected²⁶ for the missing inertial term. Diffusion theory of this kind does not lead to the correct description of the free rotor when the liquid evaporates into a dilute gas.

F. The Molecular Liquid at Room Temperature and Pressure

A combination of many careful measurements^{1,4,79-85} on liquid dichloromethane at room temperature and pressure, using microwave spectroscopy at spot frequencies and Fourier transform spectroscopy for the far infrared region produces the result of Fig. 9. This spectrum stretches over about three frequency decades and is much broader than the envelope of the free rotor absorption, the Fourier transform of Eq. (64). Figure 9 expresses the result both in terms of the far infrared power absorption coefficient and the dielectric loss, using the link provided by Eq. (6). Not only must a complete theory of diffusion describe both the microwave and far infrared data consistently in terms of the fundamental constants but it should also be able to describe all further *spectral moments*.⁸⁶⁻⁹⁰ The latter are related¹ in classical statistical mechanics to the classical acf's describing the molecu-

lar diffusion processes. Among the most prominent of these are the orientational acf, essentially the Fourier transform of the dielectric loss (zero-order spectral moment); and the rotational velocity acf which is the Fourier transform of the second moment, the power absorption coefficient. The next moment is the fourth, which is not observed directly, but which can be obtained⁸⁶⁻⁹⁰ through the product $\omega^2\alpha(\omega)$. Similarly the sixth spectral moment is $\omega^4\alpha(\omega)$ and so on. Odd spectral moments can be constructed, but are of less interest, basically because the time expansion of a classical correlation function contains only even terms.¹

The self-consistent description of zero and second spectral moments is difficult for contemporary diffusion theory. It is impossible for the original and corrected (Section I) theories of diffusion, and difficult for the itinerant oscillators, even with four parameters. The Mori and Grigolini continued fractions must be truncated at some stage, which introduce empiricism. Contemporary diffusion theory cannot come to grips at all with the many new ccf's from computer simulation⁴⁷⁻⁵⁷ which indirectly affect the spectra. The fragility of the theoretical approach is exposed by the fourth spectral moment. Approximate analytical expressions for the far infrared power absorption can be obtained¹ from the 1977 itinerant oscillator, an approximant of the Mori continued fraction, and from the improved 1987 version.⁴¹⁻⁴³ However, if these complicated expressions are simply multiplied by ω^2 to form the fourth spectral moment, they result in plateau absorption which persists indefinitely at high frequencies, an obviously unacceptable result. The fourth moment plateau is the same kind of disaster as the Debye plateau in the second moment.^{1,12} The Debye theory fails for the second moment and the itinerant oscillator for the fourth moment. Any force fitting of the itinerant oscillator is bound to unravel at the fourth moment. Similarly, higher approximants of the Mori continued fraction will fail at higher moments, according to the level of truncation.

The only theory discussed so far that maintains integrity for all spectral moments is that of the free rotor ensemble leading to Eq. (64). This is limited to the case where there is no molecular interaction.

G. Molecular Dynamics Simulation

This is a technique⁹¹ that now pervades about 40% of all the literature in physical chemistry and related disciplines. Some of its powerful results have been discussed in Section I. More details of the method will be discussed in Section 3. When faced with spectral moments, however, even this technique runs into well-defined limitations, even though it has left the traditional approach on the blocks. It is as well to describe these limitations here, and to emphasize the fundamental importance of experimental data, accurate and wide ranging, for simple molecular liquids. No

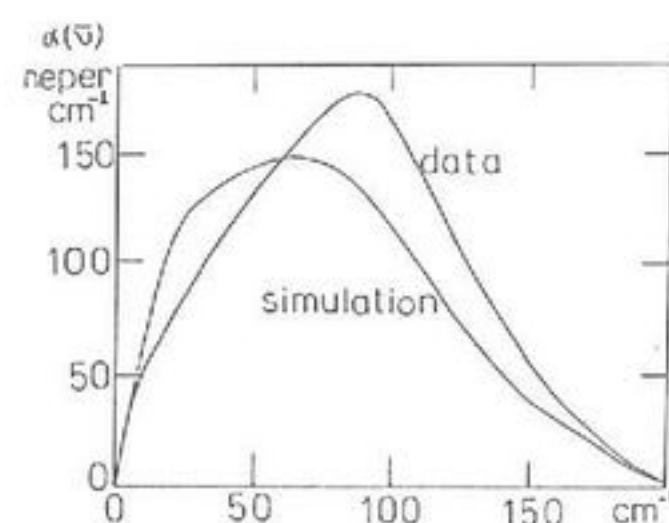


Figure 10. Computer simulation of the experimental absorption of Fig. 9. Simulation; — experimental data.

theory or numerical technique, however powerful, is the last word in natural philosophy.

Contemporary computer simulation methods rely heavily⁹¹⁻⁹⁴ on the numerical approximation of the classical equations of motion. These approximations involve expansions of fundamental dynamical variables, for example

$$r(t + \Delta t) = r(t) + \dot{r}(t)\Delta t + \frac{1}{2} \frac{F(t)\Delta t^2}{m} + O(\Delta t^3) \quad (66)$$

$$r(t - \Delta t) = r(t) - \dot{r}\Delta t + \frac{1}{2} F(t) \frac{\Delta t^2}{m} - O(\Delta t^3) \quad (67)$$

illustrating the leapfrog algorithm⁹¹ for translational motion. Here r is the position of the molecular center of mass, $F(t)$ the net force on the molecule, and m its mass. In a digital computer, with a finite storage capacity and speed, these expansions must be truncated at some order. From this it can be shown that only some of the complete set of ccf's (Section I) can be obtained numerically, depending on the order of the truncation of a series expansion such as Eqs. (66) and (67).

Figure 10 is an illustration of the match between simulation^{1,4} and far infrared absorption for dichloromethane liquid at 293 K and 1 bar. The simulated power absorption has been obtained by Fourier transforming the rotational velocity acf obtained from the dynamical trajectories generated by the 108 molecules used. The orientational acf, related to the dielectric spectrum at the lower end of the far infrared, can be obtained from the same trajectories. The close match between simulation and spectra, which can now be obtained with model or ab initio potentials, must be tempered with the realization that the simulation involves approximations. These typically include the following:

1. The success of the simulation is limited by its inherent confinement⁹¹

to the intermediate frequency range covered by the second spectral moment. Accurate definition of the frequency dependence of the fourth moment,⁸⁶⁻⁹⁰ and of higher moments, would require simulated time-correlation functions of higher derivatives of the molecular dipole moment, and because of the approximations illustrated earlier for the leapfrog algorithm, for example, these are rarely if ever available or are not defined accurately. In exceptional cases, higher-order algorithms have been used⁹⁵ to generate the required acf's for higher spectral moments, but little is known in general. Similarly, at long times, conventional computer simulation is limited by several different factors, and does not extend much further than the nanosecond range. Production of the low frequency region of the spectrum of Fig. 10 by simulation is therefore more difficult than the far infrared range.

2. The spectrum of liquid dichloromethane over the three-decade span of Fig. 9 stems from cooperative molecular dynamical processes involving ccf's between different molecules. The dielectric permittivity cannot be built up properly without sufficient consideration⁹⁷⁻¹⁰⁰ of these multimolecular effects.

Despite these limitations, computer simulation is able to build up an acceptable representation of the second moment spectrum of liquid dichloromethane without the degree of empiricism of conventional diffusion theory. Increasingly, it is possible to solve the equations of motion of a larger and larger number of moving and interacting molecules interacting with potentials modelled or computed ab initio. An analytical representation of the potential energy between two molecules as a function of intermolecular separation and relative orientation in frame, (X, Y, Z) is known¹⁰¹⁻¹⁰³ as the "pair potential" and will be described in more detail in Chapter 3. Progress is being made rapidly towards constructing the pair potential from fundamental quantum mechanical principles, and towards replacing¹⁰⁴⁻¹⁰⁶ the older model representation of the pair potential based on atom to atom Lennard-Jones parameters.

H. From Liquid to Glass at Constant Pressure

Solutions of dichloromethane in solvents such as decalin can be supercooled¹⁰⁷ well below the normal melting point at room pressure. This has the effect¹ of increasing the viscosity of the solution by several orders of magnitude. In the supercooled liquid solution of dichloromethane in decalin this has the effect^{1,107,108} of spreading the dielectric-far infrared spectrum over a vast frequency range. Not only is the peak of the zero moment spectrum (the dielectric loss) split into two and broadened considerably over the simple Debye result, but it is also removed from the peak of the